Am J Transl Res 2016;8(12):5309-5319
www.ajtr.org /ISSN:1943-8141/AJTR0040119

Original Article

Adipose-specific ablation of *Nrf2* transiently delayed high-fat diet-induced obesity by altering glucose, lipid and energy metabolism of male mice

Le Zhang[1,2], Kalavathi Dasuri[2], Sun-Ok Fernandez-Kim[2], Annadora J Bruce-Keller[2], Jeffrey N Keller[2]

[1]Institute on Aging, Department of Geriatrics, Tongji Hospital, Tongji Medical College, Huazhong University of Science and Technology, 1095 Jiefang Road, Wuhan 430030, Hubei, China; [2]Pennington Biomedical Research Center/LSU System, 6400 Perkins Road, Baton Rouge, LA 70808, USA

Received September 16, 2016; Accepted December 5, 2016; Epub December 15, 2016; Published December 30, 2016

Abstract: Nuclear factor E2-related factor 2 (NRF2) is a well-known master controller of the cellular adaptive antioxidant and detoxification response. Recent studies demonstrated altered glucose, lipid and energy metabolism in mice with a global *Nrf2* knockout. In the present study, we aim to determine the effects of an adipose-specific ablation of *Nrf2* (ASAN) on diet-induced obesity (DIO) in male mice. The 6-week-old adipose-specific *Nrf2* knockout (NK) and its *Nrf2* control (NC) mice were fed with either control diet (CD) or high-fat diet (HFD) for 14 weeks. NK mice exhibited transiently delayed body weight (BW) growth from week 5 to week 11 of HFD feeding, higher daily physical activity levels and preferential use of fat over carbohydrates as a source of energy at week 8 of the CD-feeding period. After 14 weeks of feeding, NK mice showed comparable results with NC mice with respect to the overall BW and body fat content, but exhibited reduced blood glucose, reduced number but increased size of adipocytes, accompanied with elevated expression of many genes and proteins in the visceral fat related to glucose, lipid and energy metabolism (e.g. *Fgf21*, *Pgc1a*). These results indicated that NRF2 is an important mediator for glucose, lipid and energy metabolism in adipose tissue, and ASAN could have beneficial effect for prevention of DIO during the early development of mice.

Keywords: Adipose tissue, nuclear factor E2-related factor 2 (NRF2), glucose and lipid and energy metabolism, adipose-specific ablation of Nrf2, diet-induced obesity

Introduction

White adipose tissue (WAT) has been classically defined as a reservoir for the storage and release of energy in the form of triglycerides [1]. Currently, in the context of the increasing prevalence of obesity, WAT is the largest endocrine organ and performs a variety of additional functions including secretion of numerous immune and inflammatory mediators responsible for cardiovascular disease, insulin resistance, type 2 diabetes, brain dysfunctions, breast cancer, and other effects [2-6]. Although WAT primarily comprises subcutaneous (SF) and visceral fat (VF), VF has been suggested as a more important contributor to the development of metabolic diseases [7-10], and aging is frequently accompanied by changes in total and regional fat distribution, particularly the loss of peripheral SF and accumulation of VF [8, 10]. In a previous study, we showed mild hypoxia with 38% less oxygen in the VF than in the SF of aging mice; this hypoxia was associated with a dramatic elevation of reactive oxygen species levels and significantly fewer changes in the expression of the genes involved in redox regulation [9].

Nuclear factor E2-related factor 2 (NRF2) is a transcription factor that mediates a broad-spectrum of cellular antioxidative and detoxification responses [11]. In the presence of electrophilic and oxidative stressors or chemical inducers, NRF2 is activated and translocated to the nucleus to promote the expression of a large number of antioxidant and detoxification genes by binding to the antioxidant response elements in the gene promoters [12-14].

Recently, evidence has increasingly shown that the function of NRF2 is not limited to antioxidant and detoxification effects, but has also been implicated in many other molecular processes including inflammatory responses, metabolic programming, cell proliferation, senescence and survival; however, the underlying mechanism still not completely understood [11, 14-16]. *Nrf2* ablation in wild-type and *Lep*$^{ob/ob}$ diabetic mice impaired adipogenesis and protected the mice against diet-induced obesity (DIO) [17-20], and was accompanied by reduced hepatic lipid accumulation in *Lep*$^{ob/ob}$ mice [20]. Markedly accelerated adipogenesis has also been observed in *Nrf2*$^{-/-}$ mouse embryonic fibroblasts [21].

To understand the complex roles of *Nrf2* in adipogenesis and adipose functions, and to explore whether a manipulation of adipose tissue alone could impact whole body metabolism of mice, we examined the effect of adipose-specific ablation of *Nrf2* (ASAN) on the development of obesity and associated metabolic disorders in mice in the present study.

Materials and methods

Generation and genotyping of Nrf2-knockout mice

All procedures were performed in accordance with the guidelines of the National Institutes of Health for the Care and Use of Animals and approved by the Institute Animal Care and Use Committee (IACUC) at the Pennington Biomedical Research Center. The *aP2-Cre*$^{+/-}$ mice (#005069, strain *B6*.Cg-Tg (*Fabp4-Cre*) 1Rev/J) and *Flippase recombinase*$^{+/+}$ mice (#005703, strain *B6*.Cg-Tg (*ACTFLPe*) 9205Dym/J) were obtained from The Jackson Laboratory (Sacramento, CA, USA). The targeting vectors used to generate *Nrf2*-knockout mice were purchased from the International Knockout Mouse Consortium (project #: KOMP-CSD 29871) (http://www.knockoutmouse.org/martsearch/project/29871). The strategy to generate the adipose-specific *Nrf2*-knockout mice (NK mice, *Nrf2*$^{flox/flox}$*, aP2-Cre*$^{+/-}$) and their littermate *Nrf2*-control mice (NC mice, *Nrf2*$^{flox/flox}$) is described in the Supplemental Data.

Animals and dietary treatments

Male NC and NK mice were housed in standard caging using a 12-h light/12-h dark cycle and were provided *ad libitum* access to standard rodent chow and purified water for 6 weeks. Subsequently, the mice were randomly divided at 6 weeks of age and assigned to either a high-fat diet (HFD; D12492, Research Diets, New Brunswick, NJ) or its control diet (CD; D12450B) as suggested by the manufacturer. The HFD provided 60% kcal from fat (5.55% kcal soybean oil and 54.35% kcal lard), while the CD provided 10% kcal from fat (5.55% kcal soybean oil and 4.44% kcal lard), and both diets contained the necessary mineral and vitamin mixes, with 20% kcal from protein [22]. These diets were administered for 14 weeks prior to the following experiments. Changes in body weight were measured during the CD and HFD feeding period. The total body fat and body muscle content were measured using nuclear magnetic resonance spectroscopy (Minispec, Brucker Optics, Billerica, MA).

Oxymax measurement

Metabolic measurement was performed for 1 week using mice at week 8 of the CD/HFD feeding using an Oxymax indirect calorimetry system (Columbus Instruments, Columbus, OH, USA) [23]. The mice were individually housed in the chamber with a 12-h light/12-h dark cycle at an ambient temperature of 22-24°C. The VO_2 and VCO_2 were determined using the following Oxymax system settings: air flow, 0.6 L/min; sample flow, 0.5 L/min; settling time, 6 min; and measuring time, 3 min. The system was calibrated against a standard gas mixture to measure the O_2 consumed (VO_2, mL/kg/h) and CO_2 generated (VCO_2, mL/kg/h) and to assess the physical activity of the mice (counts) over a 24-h period. The net substrate oxidation (respiratory exchange ratio, RER, VCO_2/VO_2) was calculated using the classic theory and equations of Lusk [24].

Blood glucose tolerance test

After overnight fasting, the animals received D-(+)-glucose (0.5 g/kg body weight) through intraperitoneal injection. At 30, 60 and 120 min after glucose administration, the glucose levels in the blood collected from tail bleeds were immediately analyzed. After examination, the animals were euthanized for the following studies.

Serum and tissue collection

At 20 weeks of age, the mice were fasted overnight, euthanized by isoflurane anesthesia, exsanguinated via cardiac puncture, perfused

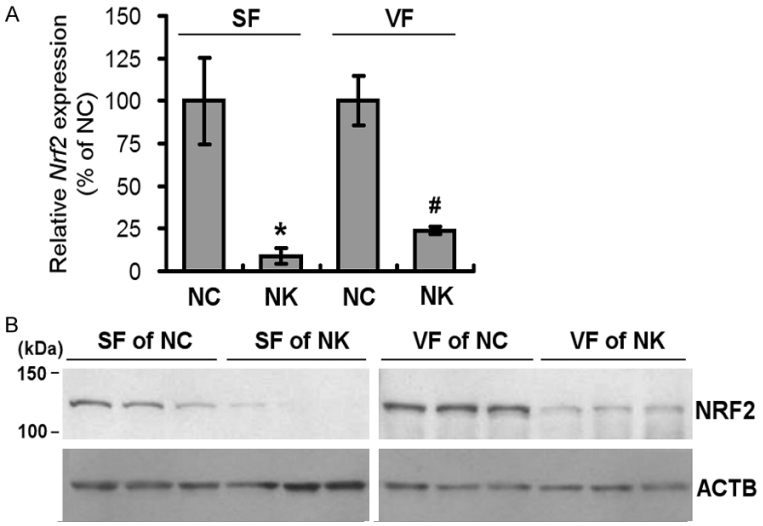

Figure 1. Confirmation of *Nrf2* knockout in the fat tissues of mice. A: Relative protein level of NRF2 in the SF and VF of NC and NK mice. B: Representative figure of the NRF2 protein expression in 3 samples of the SF and VF of NC and NK mice. Bars represent mean ± SEM, n = 6/group. *Different from NC-SF, P<0.05; #Different from NC-VF, P<0.05).

with phosphate-buffered saline (PBS, pH 8.0) and decapitated. VF (epididymal fat pads) and SF (inguinal fat pads) were collected, weighed, and subsequently divided for formalin fixation and freezing for biochemical measurements.

Plasma analysis

Blood was collected at euthanization via cardiac puncture, clotted overnight and subsequently centrifuged. The plasma was isolated and analyzed using ELISA according to the manufacturer's instructions for free fatty acid (#K612-100, BioVision, Milpitas, CA, USA), total cholesterol (#439-17501, WAKO Diagnostics, Osaka, Japan), LEPTIN (#DY498, R&D Systems, Minneapolis, MN, USA) and ADIPONECTIN (#DY1119, R&D Systems).

Histological study

The SF and VF samples were stored in formalin for 10-12 days and subsequently processed for paraffin embedding. The samples were sectioned at 5 mm and subsequently stained with hematoxylin & eosin (H&E). The slides were scanned using a Hamamatsu NanoZoomer Digital Slide Scanning System (Hamamatsu City, Japan) at 20× magnification.

Quantitative real-time PCR

Total RNA from 100 mg of mouse VF was isolated using the RNeasy Lipid Tissue Mini Kit (Qiagen, Valencia, CA). cDNA was made from 2 μg of extracted total RNA using M-MuLV transcriptase (New England Biolabs, Ipswich, MA). The quantitative real-time PCR (qPCR) was performed in a 20-μL reaction system containing 1× JumpStart™ Taq ReadyMix for qPCR (Sigma, St. Louis, MO, USA), 1× PrimeTime Pre-designed primers (IDT, Coralville, IA, USA), hydrolysis probe (6-FAM/ZEN/IBFQ mode, IDT) and 10 ng of cDNA. The qPCR was performed using an ABI PRISM 7000 system (Applied Biosystems, Foster City, CA, USA). Each sample was loaded in triplicate, and negative and positive controls were included. The amplification of *Gadph* was used as an internal reference gene. For data analysis, the $_{\Delta\Delta}C_t$ method was used.

Western blotting

Antibody anti-DLK1 was purchased from Millipore (#ABN40, Temecula, CA, USA); antibodies anti-PPARG (#2435) and anti-CEBPA (#2295) were purchased from Cell Signaling (Danvers, MA, USA); antibody anti-ACTB was obtained from Santa Cruz Biotechnology (#sc-47778, Santa Cruz, CA, USA) and used as a reference gene. The HRP-conjugated secondary antibodies were purchased from Jackson ImmunoResearch Laboratories (West Grove, PA, USA).

The protein lysates from mouse VF and SF were prepared in RIPA buffer, analyzed using SDS-PAGE and subsequently transferred to a nitrocellulose membrane. The membrane was subsequently probed with antibodies as previously described. All electrophoresis and immunoblotting reagents were purchased from Bio-Rad Laboratories (Hercules, CA, USA).

Statistical analysis

Data are presented as means ± standard errors of the means (SEMs) for the number of replicates indicated. Statistical analysis was performed by using unpaired Student's *t-test* between two selected groups, and two-way ANOVA

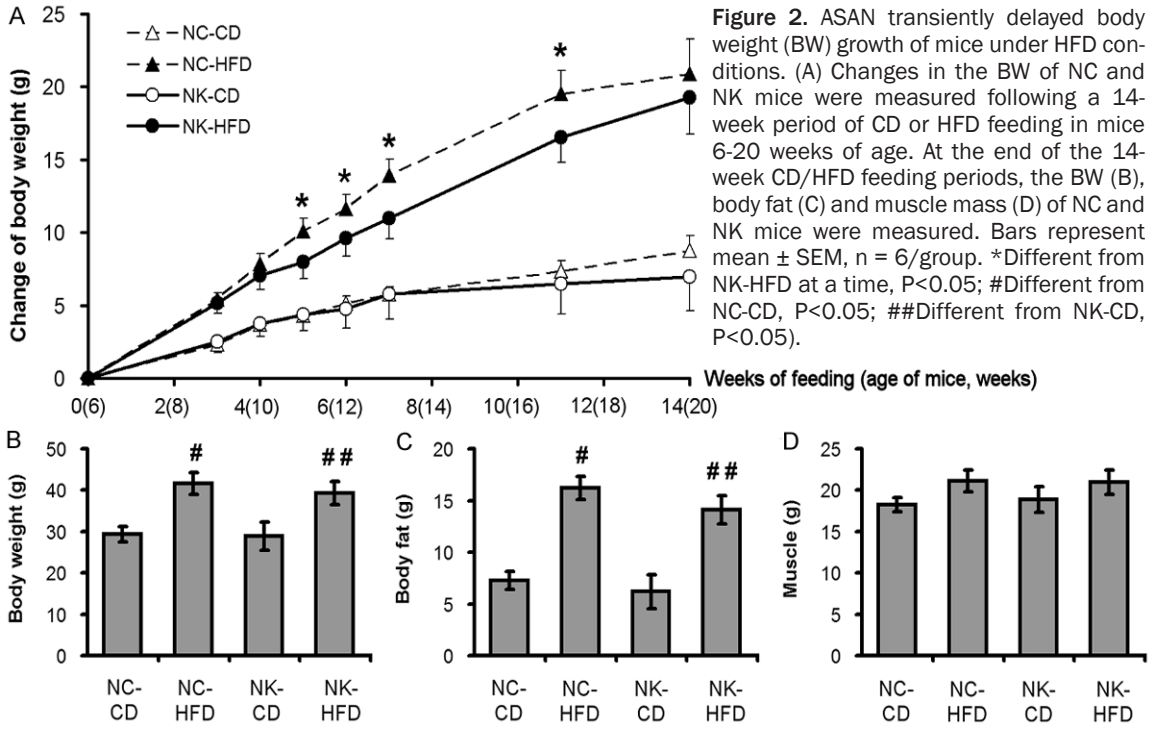

Figure 2. ASAN transiently delayed body weight (BW) growth of mice under HFD conditions. (A) Changes in the BW of NC and NK mice were measured following a 14-week period of CD or HFD feeding in mice 6-20 weeks of age. At the end of the 14-week CD/HFD feeding periods, the BW (B), body fat (C) and muscle mass (D) of NC and NK mice were measured. Bars represent mean ± SEM, n = 6/group. *Different from NK-HFD at a time, P<0.05; #Different from NC-CD, P<0.05; ##Different from NK-CD, P<0.05).

with genotype and diet as the two variables among groups (SPSS version 16.0 software). A significant difference was defined as P<0.05.

Results

Confirmation of the ablation of Nrf2 in the WAT of mice

The ablation of *Nrf2* in the WAT (SF and VF) of NK mice was confirmed using western blotting (**Figure 1**). The NRF2 protein level in NK mice was knocked down to 8.76%±4.64% and 23.89%±2.01% in the SF and VF, respectively, compared with that in NC mice. The residual NRF2 in the WAT of NK mice was primarily contributed by other cells present in the adipose tissue, such as fibroblasts, smooth muscle cells, endothelial cells, leukocytes [25], in which ASAN should not affect the expression of *Nrf2*.

Transiently delayed body weight growth of NK mice under the HFD conditions

The body weight (BW) of mice during the 14-week feeding period was measured (**Figure 2A**). Under the CD feeding conditions, no significant difference in BW changes was observed between NC and NK mice. Under the HFD feeding conditions, NK mice exhibited a substantial lower BW from week 5 to week 11 of the HFD feeding period compared with the NC mice (P<0.05), and the maximal difference was observed during weeks 7-11 of HFD feeding. At the end of the 14-week CD and HFD feeding periods, although the HFD significantly increased the BW and the body fat of both NC and NK mice, ASAN did not cause a significant difference in the mice under the same diet conditions (**Figure 2B** and **2C**). No significant difference in muscle mass was observed among all groups (**Figure 2D**).

Higher energy expenditure in NK mice

The Oxymax RER and daily physical activity (Oxymax Activity) of mice were measured at week 8 of the CD/HFD-feeding period. Under the HFD feeding conditions, the RER of both NC and NK mice varied in the range of 0.7-0.8 (**Figure 3A**), indicating that both groups of mice used fat as the main source of energy [24]. Under the CD-feeding conditions, NK mice showed lower RER throughout the measuring period compared with those of the NC mice, and the highest difference was observed during the light-off period (19:00-04:00) (P<0.05) (**Figure 3A**), indicating that NK-CD mice preferentially use fat rather than carbohydrates as sources of energy compared with NC-CD mice.

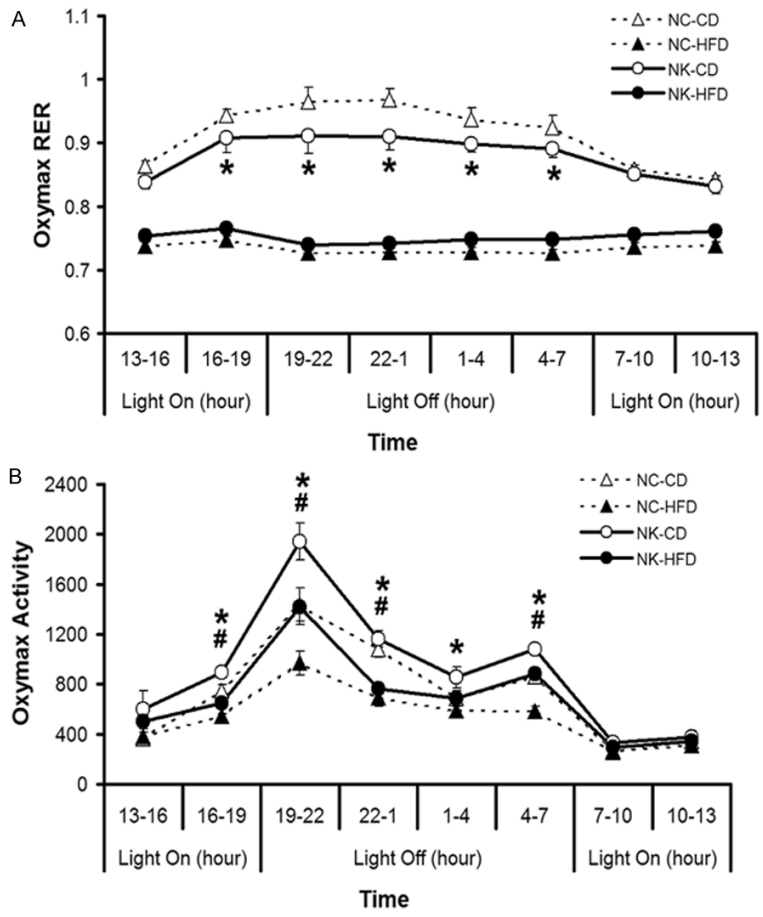

Figure 3. Increased energy expenditure resulting from ASAN in mice. The respiratory exchange ratio (RER, VCO_2/VO_2) (A) and the daily physical activity level (B) of NC and NK mice were measured at week 8 of CD/HFD feeding for 1 week using an Oxymax system. Bars represent mean ± SEM, n = 4/group. *NK-CD different from NC-CD at a time, P<0.05; #NK-HFD different from NC-HFD at a time, P<0.05.

In addition, NK mice exhibited higher physical activity levels than NC mice throughout the measuring period under both the CD and HFD conditions; the highest difference was also observed during the light-off period (P<0.05) (**Figure 3B**), consistent with the RER results.

ASAN enhanced glucose removal under the HFD conditions

After the 14-week CD or HFD feeding, the metabolic parameters of NC and NK mice were compared. The plasma cholesterol and LEPTIN levels of both NC-HFD and NK-HFD mice were significantly higher compared to their CD counterparts (**Figure 4A** and **4B**). No difference was observed in the plasma free fatty acid and ADIPONECTIN levels among all groups (**Figure 4C** and **4D**).

No significant difference in basal glucose were observed in the intraperitoneal glucose tolerance test (GTT) among all groups (**Figure 4E**), while a resistance to glucose removal 60 min after the glucose challenge was observed in NC-HFD mice compared with NC-CD mice (P<0.05). In contrast, the NK mice had a lower blood glucose level than that of the NC mice of the corresponding diet (P<0.05). Additionally, the lowest glucose level throughout the test was observed in NK-CD mice compared with all other groups (P<0.05), indicating that HFD induced resistance to glucose removal, whereas ASAN enhanced glucose removal in mice.

ASAN induced white adipocyte hypertrophy

H&E staining of adipose depots revealed that while adipocytes in the VF of NC and NK mice were significantly larger than their SF counterparts (P<0.05), larger adipocytes in both the SF and VF of NK mice were observed compared with those in NC mice (P<0.05), indicating that ASAN induced white adipocyte hypertrophy (**Figure 5**). More precisely, in SF, NC-CD adipocyte size was 87.0±9.4 μm whereas NK-CD adipocyte size was 116.4±10.9 μm; in response to HFD treatment, NC-HFD adipocyte size was 72.2±11.5 μm whereas NK-HFD had an average of 131.2±15.7 μm. In VF, NC-CD adipocyte size was 124.4±11.8 μm whereas NK-CD adipocyte size was 153.6±12.6 μm; in response to HFD treatment, NC-HFD adipocyte size was 112.8±13.4 μm whereas NK-HFD had an average of 144.3±14.1 μm.

Alterations in mRNA and protein expression in the VF of NK mice

Gene expression in the VF were examined (**Figure 6A**). HFD resulted significantly lowered

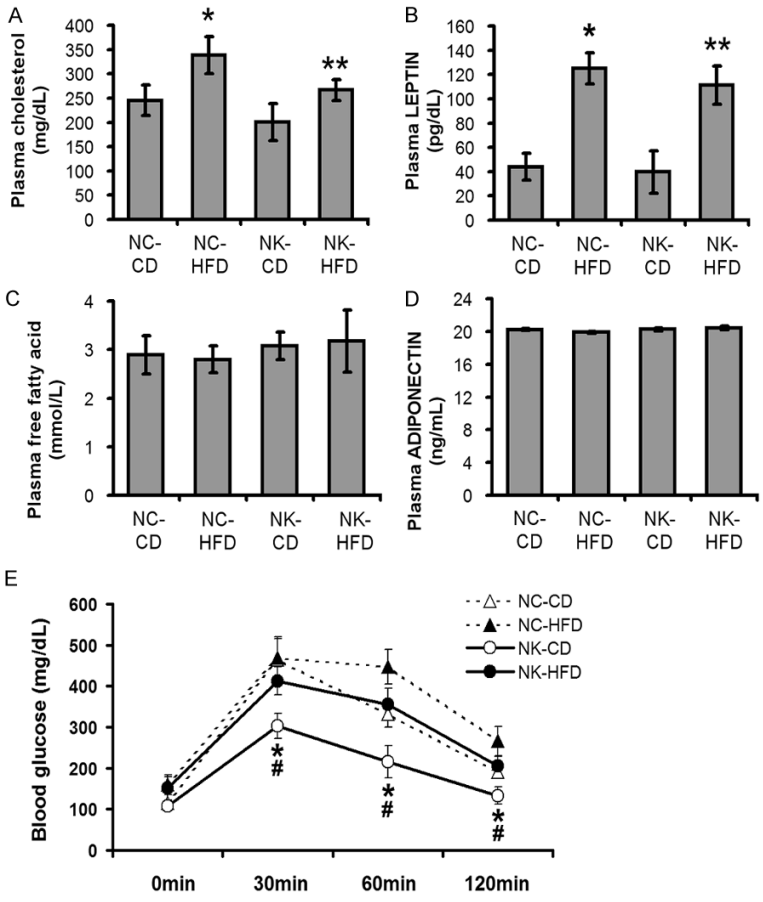

Figure 4. ASAN enhanced the glucose removal under HFD conditions. The plasma concentrations of total cholesterol (A), free fatty acid (B), LEPTIN (C) and ADIPONECTIN (D) were measured using ELISA. The intraperitoneal glucose tolerance test was performed using mice challenged with 0.5 mg/g of BW of D-(+)-glucose (E). Bars represent mean ± SEM, n = 6/group. *Different from NC-CD at a time, P<0.05; **Different from NK-CD at a time, P<0.05; #NK-HFD different from NC-HFD at a time, P<0.05.

mRNA level of *Pgc1a* and elevated mRNA levels of *Igf1*, *Fgf21*, *Insr*, *Hsl*, *Mgl*, and *Lpl* in NC mice (P<0.05). The HFD-induced higher expression of *Hsl* in NC mice (P<0.05) was not observed in NK mice.

ASAN substantially altered the gene expression in the VF of mice. The mRNA levels of *Igf1*, *Pparg* and *Lpl* were the highest in NK-HFD compared with all other groups (P<0.05), whereas the mRNA levels of *Igf1r* were the lowest in NK-HFD (P<0.05). The mRNA levels of *Pgc1a* and *El* significantly increased in the VF of NK mice compared with their diet counterparts (P<0.05). The mRNA levels of *Dlk1* and *Fgf21* in NK-HFD mice and of *Insr* and *Hsl* in NK-CD mice were significantly higher than those in NC-CD mice (P<0.05). No significant difference was observed in the mRNA levels of *Cebpa* in the VF of NC and NK mice among all groups.

On the protein level (**Figure 6B**), HFD feeding significantly induced the expression of CEBPA in the VF of NC mice (P<0.05). NK-CD mice exhibited significantly elevated DLK1, PPARG and CEBPA protein expression compared with that in NC-CD mice (P<0.05), while no significant HFD-induced difference was observed in the VF of NK mice.

Discussion

Adipogenesis

In the present study, ASAN in wild-type mice resulted in transiently delayed BW growth from week 5 to week 11 of HFD feeding in NK mice, but the BW of these mice was eventually consistent with that of NC mice at week 14 of HFD feeding. This result differed from the results of previous studies involving the complete ablation of Nrf2 in wild-type mice [17] and ASAN in *Lep*$^{ob/ob}$ diabetic mice [19, 20], in which decrease in BW and fat depots in *Nrf2* knockout mice after HFD feeding were observed. However, HFD feeding for an 8-week period in mice 4-12 weeks of age [17, 20] and an 11-week period in mice 4-15 weeks of age [19] was respectively used in these studies in contrast to the 14-week period of HFD feeding in mice 6-20 weeks of age in the present study. Within the 14-week HFD feeding period in the present study, delayed BW growth in NK mice was observed at weeks 8 and 11 of HFD feeding, consistent with the results of previous studies. Taken together, these results suggested that ASAN could transiently delay whole body weight gain in HFD-fed mice, but this benefit could be eventually suppressed after NK mice received *ad libitum* access to HFD for a long period. This result also indicated

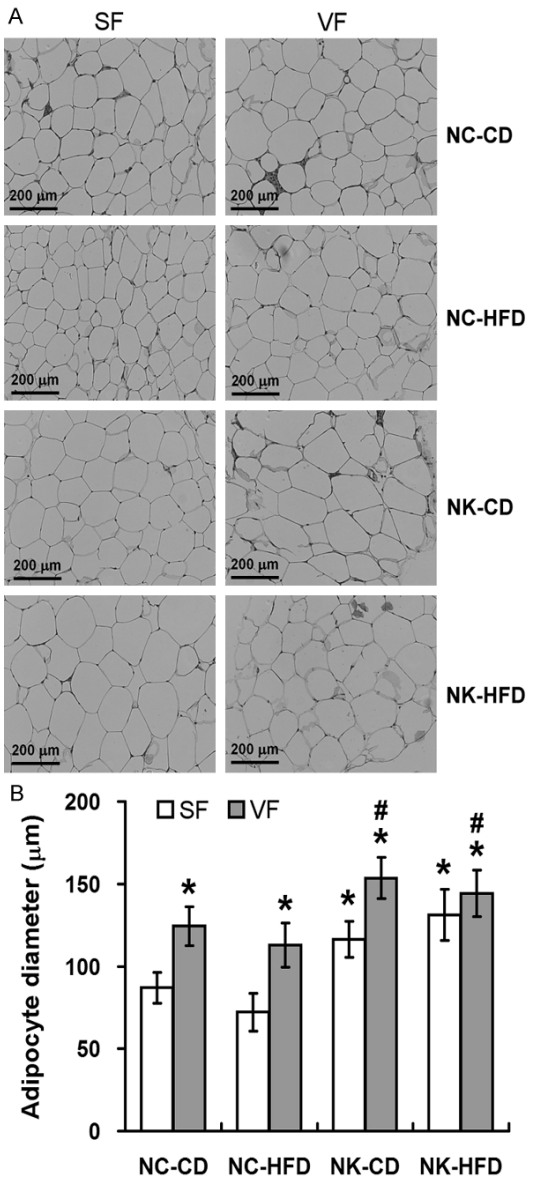

Figure 5. ASAN caused white adipocyte hypertrophy. A: H&E staining of adipocyte. B: The image quantification of the average size of adipocytes in both the SF and VF of NK mice compared with NC mice in response to CD/HFD feeding, *scale bar = 200 μm.* Bars represent mean ± SEM, n = 6/group. *Different from NC-CD of SF, P<0.05; #Different from NC-CD of VF, P<0.05.

that ASAN alone, without any restriction in the HFD access, could not completely prevent HFD-induce obesity in mice.

Adipogenesis and adipose growth are complex processes involving multiple pathways and players, including PPARG, CEBPA, IGF1/IFG1R, DLK1, and others [26, 27]. In the present study, the lowest mRNA level of *Igf1r* and the highest mRNA level of *Igf1* were observed in the VF of NK-HFD mice, suggesting that the IGF1 pathway could be involved in the NRF2 regulation of HFD-induced adipogenesis and adipose growth.

PPARG forms a positive feedback loop with CEBPA to regulate the terminal stage of adipogenesis and adipocyte maturation [26, 28]. In the present study, higher PPARG and CEBPA protein expression was observed in the VF of NK-CD mice compared with NC-CD mice, and the *Pparg* mRNA expression was also higher in NK-HFD mice than in NK-CD mice. These results might reflect the relatively larger adipocytes observed in both the VF and SF of NK mice compared with that of NC mice under both CD- or HFD-feeding conditions.

DLK1 is a key player in preadipocyte homeostasis by inhibiting preadipocyte differentiation and represses preadipocyte proliferation [29, 30]. In the present study, significantly higher *Dlk1* mRNA level was observed in the VF of NK-HFD mice compared with NC-HFD mice, and significantly elevated protein level of DLK1 was observed in NK-CD mice compared with NC-CD mice, suggesting that preadipocyte differentiation and proliferation were inhibited in NK mice.

Taken together, our results suggested that ASAN might inhibit preadipocyte differentiation and proliferation through the DLK1 pathway, while enhancing the terminal stage of adipogenesis and adipocyte maturation through the PPARG/CEBPA pathways, resulting fewer but larger-sized adipose in the WAT of NK mice at the end of the 14-week HFD feeding period.

Energy expenditure

In contrast to NK mice, NC mice used more fat as a source of energy under CD feeding conditions, and exhibited higher physical activity levels than their control-fed counterparts. At the molecular level, significantly elevated mRNA expression of *Fgf21* and *Pgc1a* was notably observed, consistent with previous studies in which the total ablation of *Nrf2* enhanced the expression of *Fgf21* in mice and that the overexpression of *Nrf2* repressed *Fgf21* expression [31, 32].

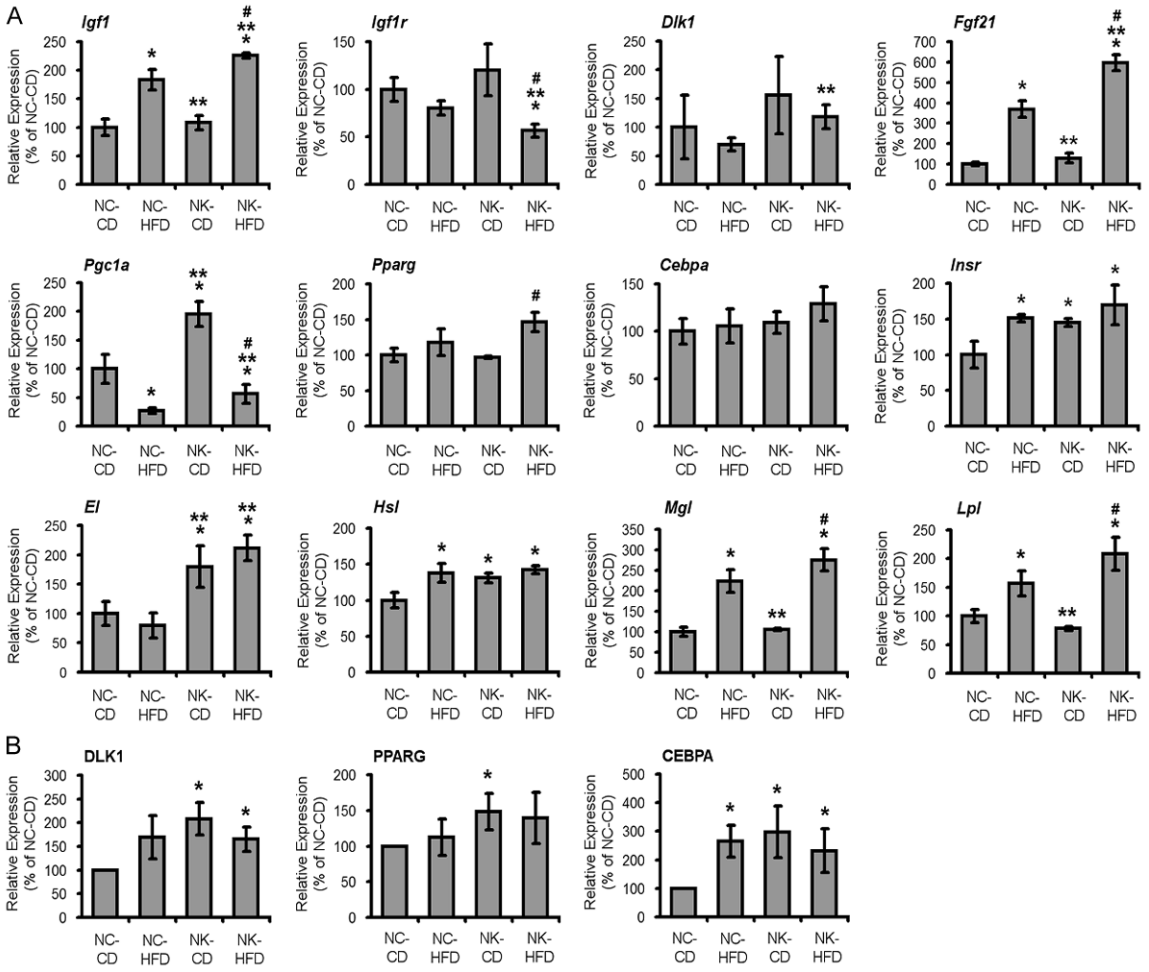

Figure 6. Diet and ASAN altered mRNA and protein expression of genes in the VF of mice. (A) mRNA level of *Igf1*, *Igf1r*, *Dlk1*, *Fgf21*, *Pgc1a*, *Pparg*, *Cebpa*, *Insr*, *El*, *Hsl*, *Mgl*, *Lpl* and (B) protein level of DLK1, PPARG, CEBPA in the VF of mice were analyzed. Abbreviation of genes: *Cebpa*, CCAAT/enhancer binding protein alpha; *Dlk1*, delta-like 1 homolog (Drosophila); *El*, endothelial lipase; *Fgf21*, fibroblast growth factor 21; *Hsl*, hormone-sensitive lipase; *Igf1*, insulin-like growth factor 1; *Igf1r*, insulin-like growth factor 1 receptor; *Insr*, insulin receptor; *Lpl*, lipoprotein lipase; *Mgl*, monoacylglycerol lipase; *Pgc1a*, peroxisome proliferator-activated receptor gamma coactivator 1-alpha; *Pparg*, peroxisome proliferator-activated receptor gamma. Bars represent mean ± SEM, n = 6/group. *Different from NC-CD, P<0.05; **Different from NC-HFD, P<0.05; #Different from NK-CD P<0.05.

FGF21 has recently been identified as a master controller that exerts a number of beneficial effects on glucose, protein, lipid and energy metabolism [33-38]. Our results further confirmed that the expression of *Fgf21* is under the control of NRF2 in the adipose tissue, suggesting a potent role of NRF2 in adipose function and metabolic regulation through FGF21 pathway.

The ADIPONECTIN and LEPTIN pathways are other classical pathways that regulate food intake and energy metabolism [4, 39]. In the present study, no significant alterations in plasma LEPTIN and ADIPONECTIN levels were observed between NC and NK mice under the same diet conditions. These results suggest that the observation of higher physical activity and preferential consumption of fat in NK mice was independent of the ADIPONECTIN and LEPTIN pathways, but could be the result of the activation of NRF2-regulated FGF21/PGC1A pathway in NK mice.

Glucose and lipid metabolism

In the present study, the *Insr* mRNA level was significantly higher in the VF of NK-CD mice

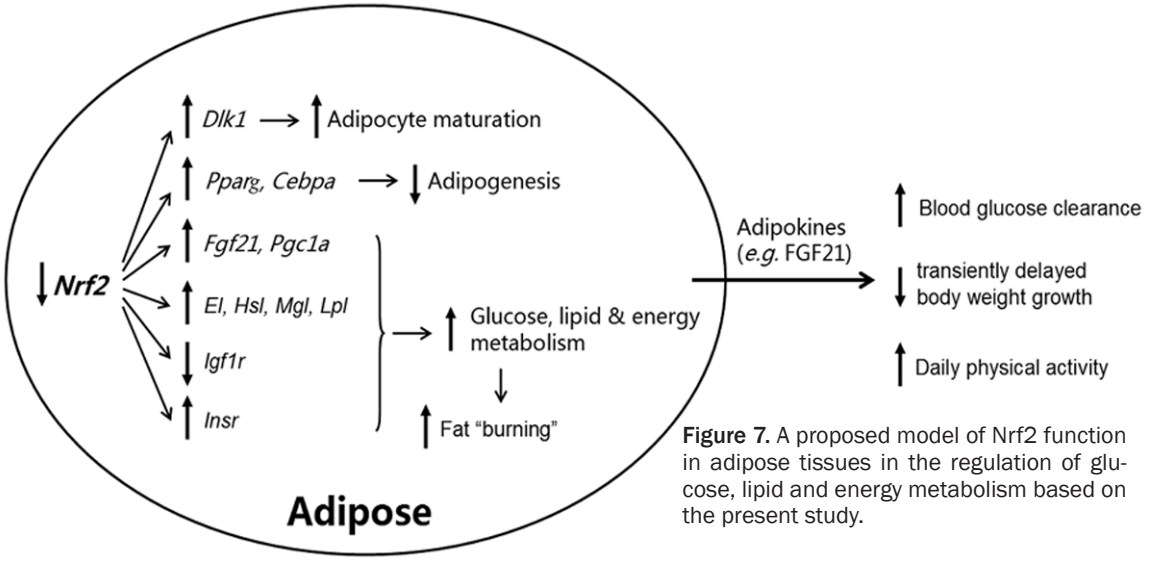

Figure 7. A proposed model of Nrf2 function in adipose tissues in the regulation of glucose, lipid and energy metabolism based on the present study.

compared with that of NC-CD mice, suggesting that insulin-stimulated glucose uptake was enhanced in the VF of NK mice, consistent with the lowered serum glucose concentration observed in NK mice.

ASAN also resulted elevated mRNA expression of lipases in the VF of mice, suggesting that ASAN facilitated the mobilization and clearance of lipids in the VF of mice [40]. Significantly higher mRNA expression of *Hsl* and *El* was observed in NK-CD mice compared with NC-CD mice, consistent with the fact that NK mice preferentially utilized fat as a source of energy compared with NC mice under CD-feeding conditions.

Function of NRF2 in adipose tissue

Effects of Nrf2 on insulin sensitivity and obesogenic regulating factors are complex. The results of the present study are consistent with those of previous studies using the *Nrf2* knockout mice [17, 19, 20] and provide additional mechanistic insights into these observations. The present study provided the first evidence that ASAN alone could transiently delay the BW growth of mice, and this delay could be eventually recovered after prolonged HFD feeding. ASAN alone resulted in the higher daily physical activity of mice, higher use of fat as a source of energy under CD-feeding conditions, altered adipogenesis and maturation, in addition to reducing blood glucose and altering the expression of genes involved in glucose, lipid and energy metabolism, indicating that NRF2 was an important mediator for glucose, lipid and energy metabolism in adipose tissue. A model of NRF2 function in adipose tissues in the regulation of glucose, lipid and energy metabolism has been proposed based on the present study (**Figure 7**).

Although ASAN is adipose specific, the phenotype changes in mice were not limited to fat tissue. Instead, the effects extended to the whole body level, reflecting the function of adipose tissue as an endocrine organ through the secretion of a variety of adipokines (e.g., FGF21). We also observed that the beneficial effects of ASAN in preventing the DIO of mice could be eventually suppressed after prolonged HFD feeding, indicating that ASAN could have beneficial effect for prevention of DIO during the early development of mice.

Disclosure of conflict of interest

None.

Authors' contribution

LZ, KD, S-OF, AJB, and JNK acquired the data and contributed to the data analysis and interpretation. LZ drafted the manuscript with contributions from all other authors. LZ and JNK contributed to the conception and design of the study, and take responsibility for the final content of the manuscript.

Address correspondence to: Le Zhang, Institute on Aging, Department of Geriatrics, Tongji Hospital, Tongji Medical College, Huazhong University of Science and Technology, 1095 Jiefang Road, Wuhan 430030, Hubei, China. Tel: +86-18802733489; E-mail: le_zhang@foxmail.com; Jeffrey N Keller, Pennington Biomedical Research Center/LSU System, 6400 Perkins Road, Baton Rouge, LA 70808, USA. Tel: +1-225-763-3190; Fax: +1-225-763-3193; E-mail: Jeffrey.Keller@pbrc.edu

References

[1] Cohen P and Spiegelman BM. Cell biology of fat storage. Mol Biol Cell 2016; 27: 2523-2527.

[2] Rosen ED and Spiegelman BM. Adipocytes as regulators of energy balance and glucose homeostasis. Nature 2006; 444: 847-853.

[3] Cleary MP and Grossmann ME. Minireview: obesity and breast cancer: the estrogen connection. Endocrinology 2009; 150: 2537-2542.

[4] Galic S, Oakhill JS and Steinberg GR. Adipose tissue as an endocrine organ. Mol Cell Endocrinol 2010; 316: 129-139.

[5] Poulos SP, Hausman DB and Hausman GJ. The development and endocrine functions of adipose tissue. Mol Cell Endocrinol 2010; 323: 20-34.

[6] Coles CA. Adipokines in healthy skeletal muscle and metabolic disease. Adv Exp Med Biol 2016; 900: 133-160.

[7] Barzilai N, She L, Liu BQ, Vuguin P, Cohen P, Wang J and Rossetti L. Surgical removal of visceral fat reverses hepatic insulin resistance. Diabetes 1999; 48: 94-98.

[8] Huffman DM and Barzilai N. Role of visceral adipose tissue in aging. Biochim Biophys Acta 2009; 1790: 1117-1123.

[9] Zhang L, Ebenezer PJ, Dasuri K, Fernandez-Kim SO, Francis J, Mariappan N, Gao Z, Ye J, Bruce-Keller AJ and Keller JN. Aging is associated with hypoxia and oxidative stress in adipose tissue: implications for adipose function. Am J Physiol Endocrinol Metab 2011; 301: E599-607.

[10] Chang SH, Beason TS, Hunleth JM and Colditz GA. A systematic review of body fat distribution and mortality in older people. Maturitas 2012; 72: 175-191.

[11] Wakabayashi N, Slocum SL, Skoko JJ, Shin S and Kensler TW. When NRF2 talks, who's listening? Antioxid Redox Signal 2010; 13: 1649-1663.

[12] Motohashi H and Yamamoto M. Nrf2-Keap1 defines a physiologically important stress response mechanism. Trends Mol Med 2004; 10: 549-557.

[13] Hybertson BM, Gao B, Bose SK and McCord JM. Oxidative stress in health and disease: the therapeutic potential of Nrf2 activation. Mol Aspects Med 2011; 32: 234-246.

[14] Huang Y, Li W, Su ZY and Kong AN. The complexity of the Nrf2 pathway: beyond the antioxidant response. J Nutr Biochem 2015; 26: 1401-1413.

[15] Chartoumpekis DV and Kensler TW. New player on an old field; the keap1/Nrf2 pathway as a target for treatment of type 2 diabetes and metabolic syndrome. Curr Diabetes Rev 2013; 9: 137-145.

[16] Uruno A, Furusawa Y, Yagishita Y, Fukutomi T, Muramatsu H, Negishi T, Sugawara A, Kensler TW and Yamamoto M. The Keap1-Nrf2 system prevents onset of diabetes mellitus. Mol Cell Biol 2013; 33: 2996-3010.

[17] Pi J, Leung L, Xue P, Wang W, Hou Y, Liu D, Yehuda-Shnaidman E, Lee C, Lau J, Kurtz TW and Chan JY. Deficiency in the nuclear factor E2-related factor-2 transcription factor results in impaired adipogenesis and protects against diet-induced obesity. J Biol Chem 2010; 285: 9292-9300.

[18] Hou Y, Xue P, Bai Y, Liu D, Woods CG, Yarborough K, Fu J, Zhang Q, Sun G, Collins S, Chan JY, Yamamoto M, Andersen ME and Pi J. Nuclear factor erythroid-derived factor 2-related factor 2 regulates transcription of CCAAT/enhancer-binding protein beta during adipogenesis. Free Radic Biol Med 2012; 52: 462-472.

[19] Xue P, Hou Y, Chen Y, Yang B, Fu J, Zheng H, Yarborough K, Woods CG, Liu D, Yamamoto M, Zhang Q, Andersen ME and Pi J. Adipose deficiency of Nrf2 in ob/ob mice results in severe metabolic syndrome. Diabetes 2013; 62: 845-854.

[20] Xu J, Donepudi AC, More VR, Kulkarni SR, Li L, Guo L, Yan B, Chatterjee T, Weintraub N and Slitt AL. Deficiency in Nrf2 transcription factor decreases adipose tissue mass and hepatic lipid accumulation in leptin-deficient mice. Obesity (Silver Spring) 2015; 23: 335-344.

[21] Shin S, Wakabayashi N, Misra V, Biswal S, Lee GH, Agoston ES, Yamamoto M and Kensler TW. NRF2 modulates aryl hydrocarbon receptor signaling: influence on adipogenesis. Mol Cell Biol 2007; 27: 7188-7197.

[22] DeFuria J, Bennett G, Strissel KJ, Perfield JW 2nd, Milbury PE, Greenberg AS and Obin MS. Dietary blueberry attenuates whole-body insulin resistance in high fat-fed mice by reducing adipocyte death and its inflammatory sequelae. J Nutr 2009; 139: 1510-1516.

[23] Xu J, Gowen L, Raphalides C, Hoyer KK, Weinger JG, Renard M, Troke JJ, Vaitheesyaran B, Lee WN, Saad MF, Sleeman MW, Teitell MA and Kurland IJ. Decreased hepatic futile cycling compensates for increased glucose dis-

posal in the Pten heterodeficient mouse. Diabetes 2006; 55: 3372-3380.
[24] Lusk G. Analysis of animal calorimetry: the oxidation of mixtures of carbohydrate and fat. J Biol Chem 1924; 59: 41-42.
[25] Suganami T and Ogawa Y. Adipose tissue macrophages: their role in adipose tissue remodeling. J Leukoc Biol 2010; 88: 33-39.
[26] Lowe CE, O'Rahilly S and Rochford JJ. Adipogenesis at a glance. J Cell Sci 2011; 124: 2681-2686.
[27] Hwa V, Fang P, Derr MA, Fiegerlova E and Rosenfeld RG. IGF-I in human growth: lessons from defects in the GH-IGF-I axis. Nestle Nutr Inst Workshop Ser 2013; 71: 43-55.
[28] Lefterova MI, Zhang Y, Steger DJ, Schupp M, Schug J, Cristancho A, Feng D, Zhuo D, Stoeckert CJ Jr, Liu XS and Lazar MA. PPARgamma and C/EBP factors orchestrate adipocyte biology via adjacent binding on a genome-wide scale. Genes Dev 2008; 22: 2941-2952.
[29] Mortensen SB, Jensen CH, Schneider M, Thomassen M, Kruse TA, Laborda J, Sheikh SP and Andersen DC. Membrane-tethered delta-like 1 homolog (DLK1) restricts adipose tissue size by inhibiting preadipocyte proliferation. Diabetes 2012; 61: 2814-2822.
[30] Traustadottir GA, Kosmina R, Sheikh SP, Jensen CH and Andersen DC. Preadipocytes proliferate and differentiate under the guidance of Delta-like 1 homolog (DLK1). Adipocyte 2013; 2: 272-275.
[31] Chartoumpekis DV, Ziros PG, Psyrogiannis AI, Papavassiliou AG, Kyriazopoulou VE, Sykiotis GP and Habeos IG. Nrf2 represses FGF21 during long-term high-fat diet-induced obesity in mice. Diabetes 2011; 60: 2465-2473.
[32] Zhang YK, Wu KC, Liu J and Klaassen CD. Nrf2 deficiency improves glucose tolerance in mice fed a high-fat diet. Toxicol Appl Pharmacol 2012; 264: 305-314.
[33] Potthoff MJ, Inagaki T, Satapati S, Ding X, He T, Goetz R, Mohammadi M, Finck BN, Mangelsdorf DJ, Kliewer SA and Burgess SC. FGF21 induces PGC-1alpha and regulates carbohydrate and fatty acid metabolism during the adaptive starvation response. Proc Natl Acad Sci U S A 2009; 106: 10853-10858.
[34] Xu J, Lloyd DJ, Hale C, Stanislaus S, Chen M, Sivits G, Vonderfecht S, Hecht R, Li YS, Lindberg RA, Chen JL, Jung DY, Zhang Z, Ko HJ, Kim JK and Veniant MM. Fibroblast growth factor 21 reverses hepatic steatosis, increases energy expenditure, and improves insulin sensitivity in diet-induced obese mice. Diabetes 2009; 58: 250-259.
[35] Chau MD, Gao J, Yang Q, Wu Z and Gromada J. Fibroblast growth factor 21 regulates energy metabolism by activating the AMPK-SIRT1-PGC-1alpha pathway. Proc Natl Acad Sci U S A 2010; 107: 12553-12558.
[36] Laeger T, Henagan TM, Albarado DC, Redman LM, Bray GA, Noland RC, Munzberg H, Hutson SM, Gettys TW, Schwartz MW and Morrison CD. FGF21 is an endocrine signal of protein restriction. J Clin Invest 2014; 124: 3913-3922.
[37] Samms RJ, Cheng CC, Kharitonenkov A, Gimeno RE and Adams AC. Overexpression of beta-Klotho in adipose tissue sensitizes male mice to endogenous FGF21 and provides protection from diet-induced obesity. Endocrinology 2016; 157: 1467-1480.
[38] Douris N, Stevanovic DM, Fisher FM, Cisu TI, Chee MJ, Nguyen NL, Zarebidaki E, Adams AC, Kharitonenkov A, Flier JS, Bartness TJ and Maratos-Flier E. Central fibroblast growth factor 21 browns white fat via sympathetic action in male mice. Endocrinology 2015; 156: 2470-2481.
[39] Karastergiou K and Mohamed-Ali V. The autocrine and paracrine roles of adipokines. Mol Cell Endocrinol 2010; 318: 69-78.
[40] Lafontan M and Langin D. Lipolysis and lipid mobilization in human adipose tissue. Prog Lipid Res 2009; 48: 275-297.

Supplemental method: generation and genotyping of adipose-specific *Nrf2*-knockout mice

All procedures were performed in accordance with the guidelines of the National Institutes of Health for the Care and Use of Animals and approved by the Institute Animal Care and Use Committee (IACUC) at the Pennington Biomedical Research Center. The *aP2-Cre*$^{+/-}$ mice of *C57bl/6* background [Stock number: 005069, strain B6.Cg-Tg (*Fabp4-Cre*) 1Rev/J] and *Flippase recombinase*$^{+/+}$ (*Flp*$^{+/+}$) mice of *C57bl/6* background [Stock number: 005703, strain B6.Cg-Tg (*ACTFLPe*) 9205Dym/J] were obtained from The Jackson Laboratory (Sacramento, CA, USA). The targeting vectors PRPGS00171_A_H03 used to generate *Nrf2*-knockout mice were purchased from the International Knockout Mouse Consortium (project #: KOMP-CSD 29871) (http://www.knockoutmouse.org/martsearch/project/29871). The vectors harbored a flippase recombinase target (FRT)-flanked region containing the *LacZ beta-Galactosidase* and *Neomycin* expression genes and a *LoxP*-flanked region containing exons 4 and 5 of mouse *Nrf2* (FRT-*Nrf2*$^{flox/+}$).

The linearized targeting vector was introduced into *C57bl/6* embryonic stem (ES) cells using electroporation. Putative homologous recombinants were selected according to ES cell growth in the presence of G418. The confirmed mutant ES cells were used to generate chimeric mice through the aggregation of mutant ES cells with E2.5 embryos, followed by the transfer of the aggregated embryos to pseudopregnant females. The obtained chimeric male was backcrossed with *C57bl/6* mice to confirm germline transmission and obtain stable FRT-*Nrf2*$^{flox/+}$ mice (Supplementary Figure 1). The FRT-*Nrf2*$^{flox/+}$ mice were first bred with *Flp*$^{+/+}$ mice to remove the FRT-flanked region and obtain *Nrf2*$^{flox/+}$ mice (step 1), and the *Nrf2*$^{flox/+}$ mice were subsequently interbred to obtain *Nrf2*$^{flox/flox}$ (step 2) or bred with *aP2-Cre*$^{+/-}$ mice to obtain *Nrf2*$^{flox/+}$, *aP2-Cre*$^{+/-}$ mice (step 3). The *Nrf2*$^{flox/flox}$, *aP2-Cre*$^{+/-}$ mice were obtained after breeding *Nrf2*$^{flox/flox}$ mice with *Nrf2*$^{flox/+}$, *aP2-Cre*$^{+/-}$ mice (step 4), followed by backcrossing with *Nrf2*$^{flox/flox}$ mice to obtain the littermates used in the present study, the adipose-specific *Nrf2*-knockout mice (NK, *Nrf2*$^{flox/flox}$, *aP2-Cre*$^{+/-}$) and *Nrf2*-control (NC, *Nrf2*$^{flox/flox}$) mice (step 5).

Genotyping was performed with PCR using genomic DNA isolated from tail snips (Supplementary Figure 2). The removal of the FTR-flanking region was verified by PCR amplification using the primer pair F1 (5'-CAA GGT GGC TCA CAA CAT CCA TAA CAA-3') and R1 (5'-GAA CCA AGG CAT GAA GAA CAG ACA GC-3'). The removal of the loxP-flanking region was verified by PCR amplification using the primer pair F2 (5'-GCT CTT CCG AAG GTC CAG AGT TCA AAT C-3') and R2 (5'-GGT TTG TCT TTC TTG AGA CAA TGA ACT GAT GG-3'). For Cre genotyping, the primers F3 (5'-GTG AAA CAG CAT TGC TGT CAC TT-3') and R3 (5'-TTC CCG CAG AAC CTG AAG ATG TT-3') were used. The primer pair F4 (5'-GCC TTC TTT TGT GTC TTG ATA GTT CGC C-3') and R4 (5'-GGA TAC TGA CCT GGG TCA TCT TTT CAC G-3') was used to detect *β-Actin* genomic DNA.

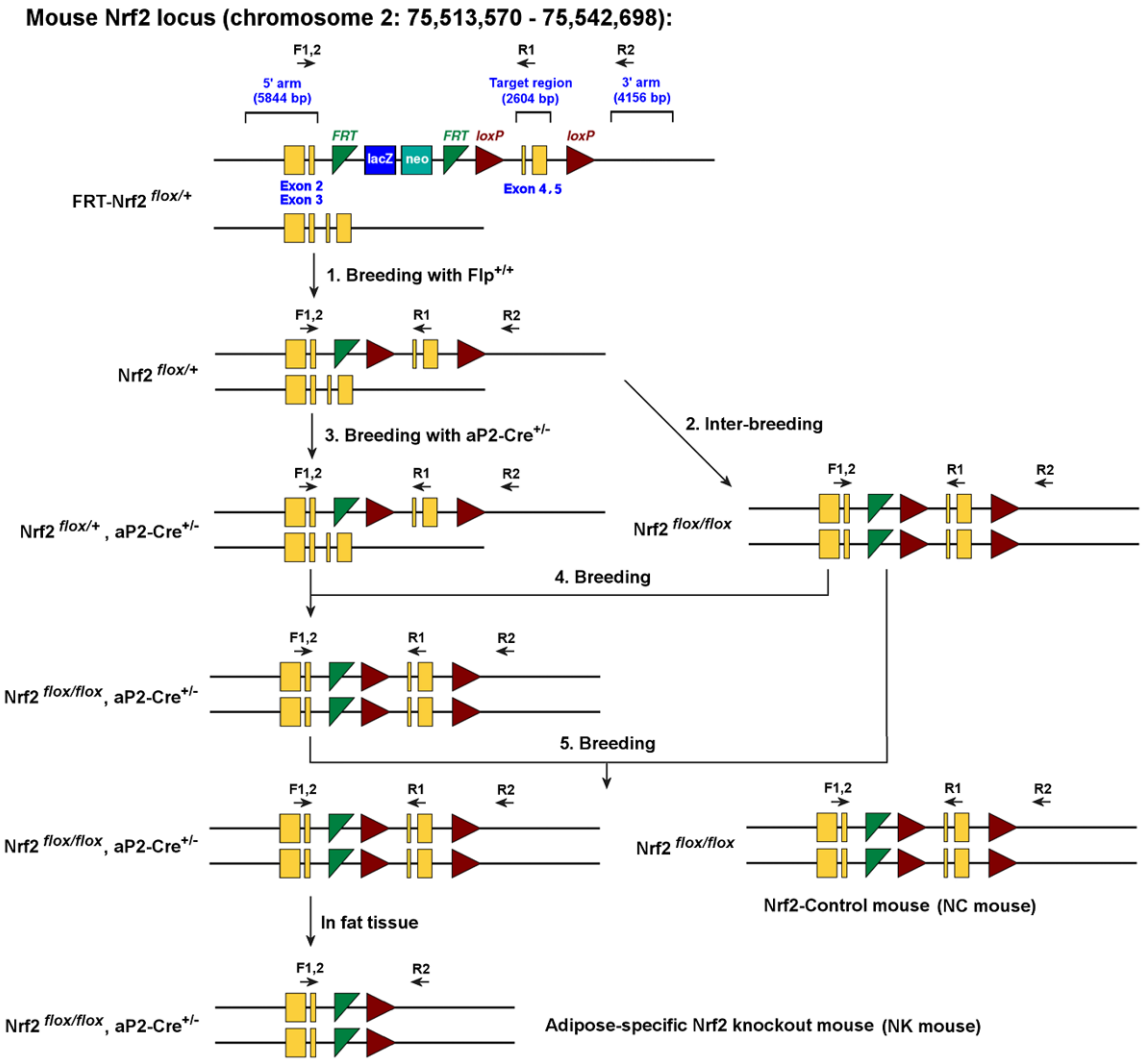

Supplementary Figure 1. Breeding strategy for the generation of adipose-specific Nrf2-knockout mouse (NK mouse) and its Nrf2-Control mouse (NC mouse).

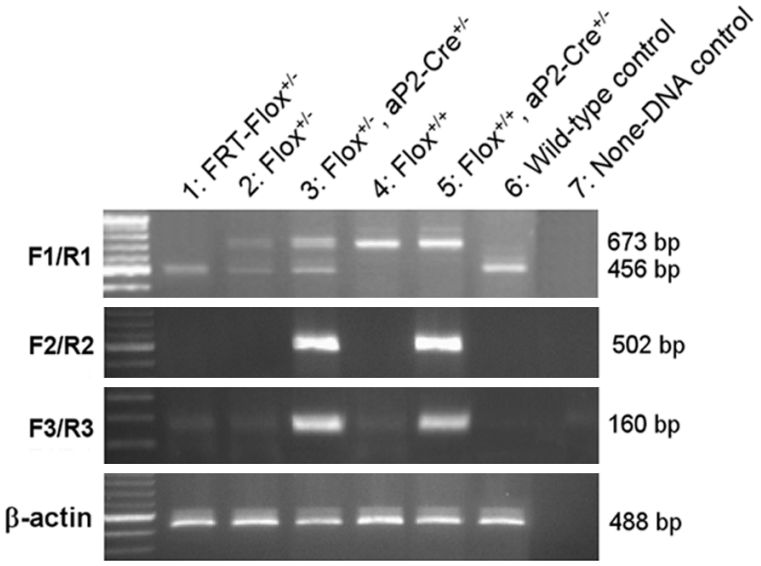

Supplementary Figure 2. Genotyping of mice for generation of the NK mice (lane 5, *Nrf2*$^{flox/flox}$, *aP2-Cre*$^{+/-}$) and NC mice (lane 4, *Nrf2*$^{flox/flox}$).